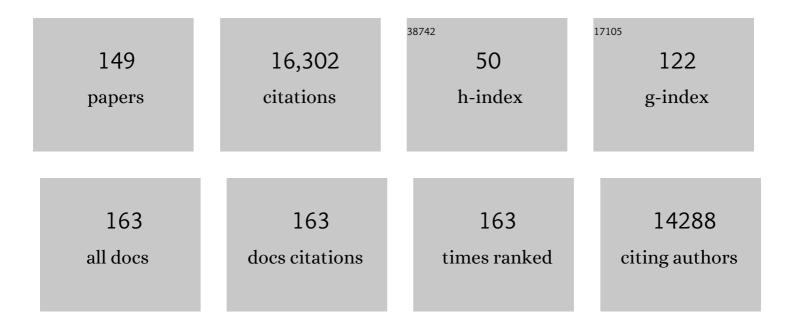
Roland Riek

List of Publications by Year in descending order

Source: https://exaly.com/author-pdf/5426581/publications.pdf Version: 2024-02-01



#	Article	IF	CITATIONS
1	Prebiotically Plausible Autocatalytic Peptide Amyloids. Chemistry - A European Journal, 2022, 28, e202103841.	3.3	10
2	Non-invasive imaging of tau-targeted probe uptake by whole brain multi-spectral optoacoustic tomography. European Journal of Nuclear Medicine and Molecular Imaging, 2022, 49, 2137-2152.	6.4	23
3	Optimization and validation of multi-state NMR protein structures using structural correlations. Journal of Biomolecular NMR, 2022, , 1.	2.8	6
4	PDBcor: An automated correlation extraction calculator for multi-state protein structures. Structure, 2022, 30, 646-652.e2.	3.3	5
5	Nanoscale Hyperspectral Imaging of Amyloid Secondary Structures in Liquid. Angewandte Chemie, 2021, 133, 4595-4600.	2.0	9
6	Prebiotic Peptide Synthesis and Spontaneous Amyloid Formation Inside a Protoâ€Cellular Compartment. Angewandte Chemie - International Edition, 2021, 60, 5561-5568.	13.8	9
7	Mass Photometry of Membrane Proteins. CheM, 2021, 7, 224-236.	11.7	39
8	Nanoscale Hyperspectral Imaging of Amyloid Secondary Structures in Liquid. Angewandte Chemie - International Edition, 2021, 60, 4545-4550.	13.8	19
9	Molecular features toward high photo-CIDNP hyperpolariztion explored through the oxidocyclization of tryptophan. Physical Chemistry Chemical Physics, 2021, 23, 6641-6650.	2.8	9
10	PrÃ b iotische Peptidâ€Synthese und spontane Amyloidâ€Bildung im Inneren eines protozelluläen Kompartiments. Angewandte Chemie, 2021, 133, 5621-5629.	2.0	2
11	Structural insights into α-synuclein monomer–fibril interactions. Proceedings of the National Academy of Sciences of the United States of America, 2021, 118, .	7.1	60
12	Large-Scale Recombinant Production of the SARS-CoV-2 Proteome for High-Throughput and Structural Biology Applications. Frontiers in Molecular Biosciences, 2021, 8, 653148.	3.5	29
13	Exploration of the close chemical space of tryptophan and tyrosine reveals importance of hydrophobicity in CW-photo-CIDNP performances. Magnetic Resonance, 2021, 2, 321-329.	1.9	5
14	Modulating α-Synuclein Liquid–Liquid Phase Separation. Biochemistry, 2021, 60, 3676-3696.	2.5	67
15	On the Entropy of a One-Dimensional Gas with and without Mixing Using Sinai Billiard. Entropy, 2021, 23, 1188.	2.2	0
16	Causality in Discrete Time Physics Derived from Maupertuis Reduced Action Principle. Entropy, 2021, 23, 1212.	2.2	4
17	Structural strains of misfolded tau protein define different diseases. Nature, 2021, 598, 264-265.	27.8	7
18	The expanding amyloid family: Structure, stability, function, and pathogenesis. Cell, 2021, 184, 4857-4873.	28.9	166

Roland Riek

#	Article	IF	CITATIONS
19	Slow-wave sleep affects synucleinopathy and regulates proteostatic processes in mouse models of Parkinson's disease. Science Translational Medicine, 2021, 13, eabe7099.	12.4	29
20	Regulation of α-synuclein by chaperones in mammalian cells. Nature, 2020, 577, 127-132.	27.8	184
21	The three-dimensional structure of human β-endorphin amyloid fibrils. Nature Structural and Molecular Biology, 2020, 27, 1178-1184.	8.2	46
22	Protein Allostery at Atomic Resolution. Angewandte Chemie - International Edition, 2020, 59, 22132-22139.	13.8	21
23	Protein Allostery at Atomic Resolution. Angewandte Chemie, 2020, 132, 22316-22323.	2.0	1
24	α-Synuclein aggregation nucleates through liquid–liquid phase separation. Nature Chemistry, 2020, 12, 705-716.	13.6	440
25	Half a century of amyloids: past, present and future. Chemical Society Reviews, 2020, 49, 5473-5509.	38.1	345
26	Protein—ligand structure determination with the NMR molecular replacement tool, NMR2. Journal of Biomolecular NMR, 2020, 74, 633-642.	2.8	8
27	Detection of cerebral tauopathy in P301L mice using high-resolution large-field multifocal illumination fluorescence microscopy. Biomedical Optics Express, 2020, 11, 4989.	2.9	22
28	In-Cell NMR of Intrinsically Disordered Proteins in Mammalian Cells. Methods in Molecular Biology, 2020, 2141, 873-893.	0.9	10
29	Nuclear Magnetic Resonance Solution Structure and Functional Behavior of the Human Proton Channel. Biochemistry, 2019, 58, 4017-4027.	2.5	21
30	Proteomics-Based Monitoring of Pathway Activity Reveals that Blocking Diacylglycerol Biosynthesis Rescues from Alpha-Synuclein Toxicity. Cell Systems, 2019, 9, 309-320.e8.	6.2	12
31	A cullin-RING ubiquitin ligase targets exogenous α-synuclein and inhibits Lewy body–like pathology. Science Translational Medicine, 2019, 11, .	12.4	30
32	Functional Amyloids. Cold Spring Harbor Perspectives in Biology, 2019, 11, a033860.	5.5	200
33	Probing Ion Binding in the Selectivity Filter of the KcsA Potassium Channel. Journal of the American Chemical Society, 2019, 141, 7391-7398.	13.7	13
34	Atto Thio 12 as a promising dye for photo-CIDNP. Journal of Chemical Physics, 2019, 151, 234201.	3.0	10
35	Carbonyl Sulfide as a Prebiotic Activation Agent for Stereo- and Sequence-Selective, Amyloid-Templated Peptide Elongation. Origins of Life and Evolution of Biospheres, 2019, 49, 213-224.	1.9	4
36	Rational Structureâ€Based Design of Fluorescent Probes for Amyloid Folds. ChemBioChem, 2019, 20, 1161-1166.	2.6	5

#	Article	IF	CITATIONS
37	Two new polymorphic structures of human full-length alpha-synuclein fibrils solved by cryo-electron microscopy. ELife, 2019, 8, .	6.0	220
38	A prebiotic template-directed peptide synthesis based on amyloids. Nature Communications, 2018, 9, 234.	12.8	61
39	NOEâ€Đerived Methyl Distances from a 360â€kDa Proteasome Complex. Chemistry - A European Journal, 2018, 24, 2270-2276.	3.3	9
40	Quantitative mass imaging of single biological macromolecules. Science, 2018, 360, 423-427.	12.6	453
41	Binding of Polythiophenes to Amyloids: Structural Mapping of the Pharmacophore. ACS Chemical Neuroscience, 2018, 9, 475-481.	3.5	31
42	Cooperative Induction of Ordered Peptide and Fatty Acid Aggregates. Biophysical Journal, 2018, 115, 2336-2347.	0.5	10
43	Lipid- and Cholesterol-Mediated Time-Scale-Specific Modulation of the Outer Membrane Protein X Dynamics in Lipid Bilayers. Journal of the American Chemical Society, 2018, 140, 15402-15411.	13.7	23
44	15N transverse relaxation measurements for the characterization of µs–ms dynamics are deteriorated by the deuterium isotope effect on 15N resulting from solvent exchange. Journal of Biomolecular NMR, 2018, 72, 125-137.	2.8	8
45	Structure and dynamics conspire in the evolution of affinity between intrinsically disordered proteins. Science Advances, 2018, 4, eaau4130.	10.3	38
46	Cryo-EM structure of alpha-synuclein fibrils. ELife, 2018, 7, .	6.0	444
47	Femtosecond X-ray coherent diffraction of aligned amyloid fibrils on low background graphene. Nature Communications, 2018, 9, 1836.	12.8	34
48	Peptide Amyloids in the Origin of Life. Journal of Molecular Biology, 2018, 430, 3735-3750.	4.2	75
49	Amyloid Fibril Polymorphism: Almost Identical on the Atomic Level, Mesoscopically Very Different. Journal of Physical Chemistry B, 2017, 121, 1783-1792.	2.6	41
50	α-Synuclein lipoprotein nanoparticles. Nanotechnology Reviews, 2017, 6, 105-110.	5.8	7
51	Fast NMRâ€Based Determination of the 3D Structure of the Binding Site of Protein–Ligand Complexes with Weak Affinity Binders. Angewandte Chemie, 2017, 129, 5292-5295.	2.0	2
52	Lipid Internal Dynamics Probed in Nanodiscs. ChemPhysChem, 2017, 18, 2651-2657.	2.1	47
53	Fast NMRâ€Based Determination of the 3D Structure of the Binding Site of Protein–Ligand Complexes with Weak Affinity Binders. Angewandte Chemie - International Edition, 2017, 56, 5208-5211.	13.8	21
54	Solution structure of discoidal high-density lipoprotein particles with a shortened apolipoprotein A-I. Nature Structural and Molecular Biology, 2017, 24, 187-193.	8.2	105

#	Article	IF	CITATIONS
55	Highâ€density lipoproteinâ€like particle formation of Synuclein variants. FEBS Letters, 2017, 591, 304-311.	2.8	17
56	Emerging Structural Understanding of Amyloid Fibrils by Solid-State NMR. Trends in Biochemical Sciences, 2017, 42, 777-787.	7.5	73
57	eNORA2 Exact NOE Analysis Program. Journal of Chemical Theory and Computation, 2017, 13, 4336-4346.	5.3	32
58	Proton-Detected NMR Spectroscopy of Nanodisc-Embedded Membrane Proteins: MAS Solid-State vs Solution-State Methods. Journal of Physical Chemistry B, 2017, 121, 7671-7680.	2.6	23
59	The Three-Dimensional Structures of Amyloids. Cold Spring Harbor Perspectives in Biology, 2017, 9, a023572.	5.5	48
60	Micelles, Bicelles, and Nanodiscs: Comparing the Impact of Membrane Mimetics on Membrane Protein Backbone Dynamics. Angewandte Chemie - International Edition, 2017, 56, 380-383.	13.8	86
61	Quenched hydrogen-deuterium exchange NMR of a disease-relevant Aβ(1-42) amyloid polymorph. PLoS ONE, 2017, 12, e0172862.	2.5	6
62	Structures of the First Extracellular Domain of CRF Receptors. Current Molecular Pharmacology, 2017, 10, 318-324.	1.5	0
63	More than a Rumor Spreads in Parkinson's Disease. Frontiers in Human Neuroscience, 2016, 10, 608.	2.0	11
64	Solid-state NMR sequential assignment of an Amyloid-β(1–42) fibril polymorph. Biomolecular NMR Assignments, 2016, 10, 269-276.	0.8	18
65	S-Nitrosylation Induces Structural and Dynamical Changes in a Rhodanese Family Protein. Journal of Molecular Biology, 2016, 428, 3737-3751.	4.2	12
66	The Dynamic Basis for Signal Propagation in Human Pin1-WW. Structure, 2016, 24, 1464-1475.	3.3	20
67	Amyloid Aggregates Arise from Amino Acid Condensations under Prebiotic Conditions. Angewandte Chemie, 2016, 128, 11781-11785.	2.0	22
68	Amyloid Aggregates Arise from Amino Acid Condensations under Prebiotic Conditions. Angewandte Chemie - International Edition, 2016, 55, 11609-11613.	13.8	65
69	Atomic-resolution structure of a disease-relevant Aβ(1–42) amyloid fibril. Proceedings of the National Academy of Sciences of the United States of America, 2016, 113, E4976-84.	7.1	712
70	The activities of amyloids from a structural perspective. Nature, 2016, 539, 227-235.	27.8	386
71	Solid-state NMR sequential assignment of the β-endorphin peptide in its amyloid form. Biomolecular NMR Assignments, 2016, 10, 259-268.	0.8	5
72	The HET-S/s Prion Motif in the Control of Programmed Cell Death. Cold Spring Harbor Perspectives in Biology, 2016, 8, a023515.	5.5	40

#	Article	IF	CITATIONS
73	NMR-Based Determination of the 3D Structure of the Ligand–Protein Interaction Site without Protein Resonance Assignment. Journal of the American Chemical Society, 2016, 138, 4393-4400.	13.7	46
74	Preparation and Characterization of Stable α-Synuclein Lipoprotein Particles. Journal of Biological Chemistry, 2016, 291, 8516-8527.	3.4	49
75	The Exact NOE as an Alternative in Ensemble Structure Determination. Biophysical Journal, 2016, 110, 113-126.	0.5	39
76	Dynamic Assembly and Disassembly of Functional β-Endorphin Amyloid Fibrils. Journal of the American Chemical Society, 2016, 138, 846-856.	13.7	71
77	The Neurite Outgrowth Inhibitory Nogo-A-Δ20 Region Is an Intrinsically Disordered Segment Harbouring Three Stretches with Helical Propensity. PLoS ONE, 2016, 11, e0161813.	2.5	2
78	Compiled data set of exact NOE distance limits, residual dipolar couplings and scalar couplings for the protein GB3. Data in Brief, 2015, 5, 99-106.	1.0	11
79	A Structural Ensemble for the Enzyme Cyclophilin Reveals an Orchestrated Mode of Action at Atomic Resolution. Angewandte Chemie - International Edition, 2015, 54, 11657-11661.	13.8	30
80	α-Synuclein Insertion into Supported Lipid Bilayers As Seen by in Situ X-ray Reflectivity. ACS Chemical Neuroscience, 2015, 6, 374-379.	3.5	7
81	Solution NMR Studies of Recombinant Aβ(1–42): From the Presence of a Micellar Entity to Residual βâ€ S heet Structure in the Soluble Species. ChemBioChem, 2015, 16, 659-669.	2.6	42
82	Structure based aggregation studies reveal the presence of helix-rich intermediate during α-Synuclein aggregation. Scientific Reports, 2015, 5, 9228.	3.3	172
83	Extending the eNOE data set of large proteins by evaluation of NOEs with unresolved diagonals. Journal of Biomolecular NMR, 2015, 62, 63-69.	2.8	23
84	Toxicity of Eosinophil MBP Is Repressed by Intracellular Crystallization and Promoted by Extracellular Aggregation. Molecular Cell, 2015, 57, 1011-1021.	9.7	88
85	Uncovering the Mechanism of Aggregation of Human Transthyretin. Journal of Biological Chemistry, 2015, 290, 28932-28943.	3.4	117
86	Complementarity and congruence between exact NOEs and traditional NMR probes for spatial decoding of protein dynamics. Journal of Structural Biology, 2015, 191, 306-317.	2.8	19
87	Towards Prebiotic Catalytic Amyloids Using High Throughput Screening. PLoS ONE, 2015, 10, e0143948.	2.5	67
88	Expression and Functional Characterization of Membrane-Integrated Mammalian Corticotropin Releasing Factor Receptors 1 and 2 in Escherichia coli. PLoS ONE, 2014, 9, e84013.	2.5	10
89	Contribution of Specific Residues of the β-Solenoid Fold to HET-s Prion Function, Amyloid Structure and Stability. PLoS Pathogens, 2014, 10, e1004158.	4.7	45
90	Heterodimerization of p45–p75 Modulates p75 Signaling: Structural Basis and Mechanism of Action. PLoS Biology, 2014, 12, e1001918.	5.6	21

#	Article	IF	CITATIONS
91	Intermolecular Detergent–Membrane Protein NOEs for the Characterization of the Dynamics of Membrane Protein–Detergent Complexes. Journal of Physical Chemistry B, 2014, 118, 14288-14301.	2.6	5
92	Towards a true protein movie: A perspective on the potential impact of the ensemble-based structure determination using exact NOEs. Journal of Magnetic Resonance, 2014, 241, 53-59.	2.1	31
93	Measuring membrane protein bond orientations in nanodiscs via residual dipolar couplings. Protein Science, 2014, 23, 851-856.	7.6	32
94	The production of recombinant 15N, 13C-labelled somatostatin 14 for NMR spectroscopy. Protein Expression and Purification, 2014, 99, 78-86.	1.3	1
95	Solution NMR Structure and Functional Analysis of the Integral Membrane Protein YgaP from Escherichia coli. Journal of Biological Chemistry, 2014, 289, 23482-23503.	3.4	16
96	The Presence of an Air–Water Interface Affects Formation and Elongation of α-Synuclein Fibrils. Journal of the American Chemical Society, 2014, 136, 2866-2875.	13.7	229
97	Multiple-state ensemble structure determination from eNOE spectroscopy. Molecular Physics, 2013, 111, 437-454.	1.7	28
98	Polychromatic frequency encoding in indirect dimensions in NMR spectroscopy. Molecular Physics, 2013, 111, 765-770.	1.7	0
99	Stereospecific assignments in proteins using exact NOEs. Journal of Biomolecular NMR, 2013, 57, 211-218.	2.8	16
100	On-Surface Aggregation of α-Synuclein at Nanomolar Concentrations Results in Two Distinct Growth Mechanisms. ACS Chemical Neuroscience, 2013, 4, 408-417.	3.5	61
101	Superresolution Imaging of Amyloid Fibrils with Binding-Activated Probes. ACS Chemical Neuroscience, 2013, 4, 1057-1061.	3.5	75
102	Detergent/Nanodisc Screening for High-Resolution NMR Studies of an Integral Membrane Protein Containing a Cytoplasmic Domain. PLoS ONE, 2013, 8, e54378.	2.5	38
103	Structure-Activity Relationship of Amyloids. Research and Perspectives in Alzheimer's Disease, 2013, , 33-46.	0.1	0
104	The Mechanism of Toxicity in HET-S/HET-s Prion Incompatibility. PLoS Biology, 2012, 10, e1001451.	5.6	123
105	Relaxation Matrix Analysis of Spin Diffusion for the NMR Structure Calculation with eNOEs. Journal of Chemical Theory and Computation, 2012, 8, 3483-3492.	5.3	47
106	Discrete Three-dimensional Representation of Macromolecular Motion from eNOE-based Ensemble Calculation. Chimia, 2012, 66, 787.	0.6	10
107	On the Possible Amyloid Origin of Protein Folds. Journal of Molecular Biology, 2012, 421, 417-426.	4.2	119
108	Spatial elucidation of motion in proteins by ensemble-based structure calculation using exact NOEs. Nature Structural and Molecular Biology, 2012, 19, 1053-1057.	8.2	92

#	Article	IF	CITATIONS
109	Structural Studies of Amyloids by Quenched Hydrogen–Deuterium Exchange by NMR. Methods in Molecular Biology, 2012, 849, 185-198.	0.9	11
110	Editorial. Chimia, 2012, 66, 730-731.	0.6	0
111	Mechanism of Membrane Interaction and Disruption by α-Synuclein. Journal of the American Chemical Society, 2011, 133, 19366-19375.	13.7	198
112	Temperature Dependence of1HN–1HNDistances in Ubiquitin As Studied by Exact Measurements of NOEs. Journal of Physical Chemistry B, 2011, 115, 7648-7660.	2.6	16
113	Very simple combination of TROSY, CRINEPT and multiple quantum coherence for signal enhancement in an HN(CO)CA experiment for large proteins. Journal of Magnetic Resonance, 2011, 209, 310-314.	2.1	10
114	In vivo demonstration that α-synuclein oligomers are toxic. Proceedings of the National Academy of Sciences of the United States of America, 2011, 108, 4194-4199.	7.1	1,252
115	A Receptor-based Switch that Regulates Anthrax Toxin Pore Formation. PLoS Pathogens, 2011, 7, e1002354.	4.7	29
116	Side chain: backbone projections in aromatic and ASX residues from NMR cross-correlated relaxation. Journal of Biomolecular NMR, 2010, 46, 135-147.	2.8	9
117	Biology of Amyloid: Structure, Function, andÂRegulation. Structure, 2010, 18, 1244-1260.	3.3	496
118	Protocols for the Sequential Solidâ€State NMR Spectroscopic Assignment of a Uniformly Labeled 25 kDa Protein: HETâ€s(1â€227). ChemBioChem, 2010, 11, 1543-1551.	2.6	126
119	Multidimensional Structure–Activity Relationship of a Protein in Its Aggregated States. Angewandte Chemie - International Edition, 2010, 49, 3904-3908.	13.8	54
120	Quantitative determination of NOE rates in perdeuterated and protonated proteins: Practical and theoretical aspects. Journal of Magnetic Resonance, 2010, 204, 290-302.	2.1	32
121	Cotranslational structure acquisition of nascent polypeptides monitored by NMR spectroscopy. Proceedings of the National Academy of Sciences of the United States of America, 2010, 107, 9111-9116.	7.1	83
122	Identifying the amylome, proteins capable of forming amyloid-like fibrils. Proceedings of the National Academy of Sciences of the United States of America, 2010, 107, 3487-3492.	7.1	708
123	Transnitrosylation of XIAP Regulates Caspase-Dependent Neuronal Cell Death. Molecular Cell, 2010, 39, 184-195.	9.7	162
124	Structure–activity relationship of amyloid fibrils. FEBS Letters, 2009, 583, 2610-2617.	2.8	114
125	Mistic: Cellular localization, solution behavior, polymerization, and fibril formation. Protein Science, 2009, 18, 1564-1570.	7.6	19
126	Exact Distances and Internal Dynamics of Perdeuterated Ubiquitin from NOE Buildups. Journal of the American Chemical Society, 2009, 131, 17215-17225.	13.7	91

#	Article	IF	CITATIONS
127	Functional Amyloids As Natural Storage of Peptide Hormones in Pituitary Secretory Granules. Science, 2009, 325, 328-332.	12.6	903
128	Infectious and Noninfectious Amyloids of the HETâ€s(218–289) Prion Have Different NMR Spectra. Angewandte Chemie - International Edition, 2008, 47, 5839-5841.	13.8	51
129	Amyloid Fibrils of the HET-s(218–289) Prion Form a β Solenoid with a Triangular Hydrophobic Core. Science, 2008, 319, 1523-1526.	12.6	928
130	Bacterial Inclusion Bodies Contain Amyloid-Like Structure. PLoS Biology, 2008, 6, e195.	5.6	189
131	Amyloid as a Depot for the Formulation of Long-Acting Drugs. PLoS Biology, 2008, 6, e17.	5.6	196
132	The fold of α-synuclein fibrils. Proceedings of the National Academy of Sciences of the United States of America, 2008, 105, 8637-8642.	7.1	499
133	Conformational dynamics of the KcsA potassium channel governs gating properties. Nature Structural and Molecular Biology, 2007, 14, 1089-1095.	8.2	121
134	NMR TECHNIQUES FOR VERY LARGE PROTEINS AND RNAS IN SOLUTION. Annual Review of Biophysics and Biomolecular Structure, 2006, 35, 319-342.	18.3	95
135	Novel sst2-Selective Somatostatin Agonists. Three-Dimensional Consensus Structure by NMR. Journal of Medicinal Chemistry, 2006, 49, 4487-4496.	6.4	49
136	Infectious Alzheimer's disease?. Nature, 2006, 444, 429-431.	27.8	31
137	Fast multidimensional NMR spectroscopy by spin-state selective off-resonance decoupling (SITAR). Magnetic Resonance in Chemistry, 2006, 44, S196-S205.	1.9	10
138	Correlation of structural elements and infectivity of the HET-s prion. Nature, 2005, 435, 844-848.	27.8	433
139	High-Resolution Solid-State NMR Spectroscopy of the Prion Protein HET-s in Its Amyloid Conformation. Angewandte Chemie - International Edition, 2005, 44, 2441-2444.	13.8	109
140	3D structure of Alzheimer's amyloid-β(1–42) fibrils. Proceedings of the National Academy of Sciences of the United States of America, 2005, 102, 17342-17347.	7.1	1,859
141	NMR Structure of Mistic, a Membrane-Integrating Protein for Membrane Protein Expression. Science, 2005, 307, 1317-1321.	12.6	234
142	3d Trosy-HncaCodedcb and Trosy-HncaCodedco Experiments: Triple Resonance nmr Experiments With two Sequential Connectivity Pathways and High Sensitivity. Journal of Biomolecular NMR, 2004, 28, 289-294.	2.8	11
143	Chemical shift-dependent apparent scalar couplings: an alternative concept of chemical shift monitoring in multi-dimensional NMR experiments. Journal of Biomolecular NMR, 2003, 25, 281-290.	2.8	8
144	Three-dimensional structures of the prion protein and its doppel. Clinics in Laboratory Medicine, 2003, 23, 209-225.	1.4	5

#	Article	IF	CITATIONS
145	Novel sst4-Selective Somatostatin (SRIF) Agonists. 4. Three-Dimensional Consensus Structure by NMR. Journal of Medicinal Chemistry, 2003, 46, 5606-5618.	6.4	32
146	Pseudomultidimensional NMR by Spin-State Selective Off-Resonance Decoupling. Journal of the American Chemical Society, 2003, 125, 16104-16113.	13.7	23
147	NMR studies in aqueous solution fail to identify significant conformational differences between the monomeric forms of two Alzheimer peptides with widely different plaque-competence, Al²(1-40)oxand Al²(1-42)ox. FEBS Journal, 2001, 268, 5930-5936.	0.2	209
148	PDBcor: An Automated Correlation Extraction Calculator for Multi-State Protein Structures. SSRN Electronic Journal, 0, , .	0.4	1
149	S-Sulfhydration of the Catalytic Cysteine in the Rhodanese Domain of YgaP is Complex Dynamic Process. Matters, 0, , .	1.0	1